Investigation of the Mechanical Properties of Nano-Scale Metallic Crystal Structural with Point Defects

Chao-Jen Huang, Chan-Yen Chou, Chung-Jung Wu, Kuo-Ning Chiang

Investigation of the Mechanical Properties of Nano-Scale Metallic Crystal Structural with Point Defects

Chao-Jen Huang[1], Chan-Yen Chou[1], Chung-Jung Wu[1], and Kuo-Ning Chiang[2]

Advanced Microsystem Packaging and Nano-Mechanics Research Lab
Dept. of Power Mechanical Engineering
National Tsing Hua University
101, Sec. 2, Kuang-Fu Rd.,
Hsinchu, Taiwan 300, R.O.C.

ABSTRACT

It is difficult to know if a nano-structure has similar characteristics with bulk structure properties. Hence, this paper developed atomistic-continuum mechanics (ACM), and used the finite element method (FEM) to transfer an originally discrete atomic structure into an equilibrium continuum model. The purpose of this research is to study the Young's modulus of copper in nano-scale structure under tensile testing and vibration loading. In this approach, the face-centered-cubic (fcc) metal bonds might be able to describe the inter-atomic forces between adjacent atoms. In short, the bond of the atomic lattice could be replaced by the spring element. The mechanical properties are discussed in terms of change in the structural size and the percentage of point defects of copper.

1. INTRODUCTION

During the last few decades, many studies have been focused on the notable mechanical properties of nano-scale crystal structures, especially the properties of their Young's modulus. To date, however, no measurement systems are accurate enough to describe the physical behavior of nanostructure properties. For this reason, researchers have developed a renewed interest in the field of potential function to describe diatomic interaction. Shenoy et al. [1] offered a mixed atomistic and continuum method for materials analysis. Girifalco and Weizer [2] noted that the crystal properties, in terms of the Morse function, calculated the Morse potential parameters for cubic metals using the experimental values of the energy of vaporization, the lattice constant, and the compressibility. Rottler et al. [3] have presented an analysis of the time evolution of the self-interstitial atom and vacancy point defect populations in pure bcc metals under constant irradiation flux conditions. Chiang et al. [4] have proposed an atomic-level single-lattice method with a closed-form equation that is presented to predict the elastic characteristics of bulk metals.

The current study uses finite element methods (FEM) and the atomistic-continuum mechanics method (ACM) [5-6] to explore Young's modulus and the size effect of nanostructures. In view of the preceding research proposed, three major sets of research questions are addressed in this study as follows: First, the single-spring-single-lattice (SSSL) [4] was applied to calculate the analytical solution for a variety of metals. Second, this study explores how the size effect controls the structure's Young's modulus. Third, the result has considered the structure with point defects to compare the Young's modulus under tensile and vibration analysis. Furthermore, the research discussed the relationship between the point defects distribution and Young's modulus. In this article, an equivalent-spring structure is represented. A spring element is applied to transform the metallic bonds in order to describe the interatomic force between adjacent metallic bonds. Moreover, the originally discrete atomic structure is analyzed in the continuum level.

2. FUNDAMENTAL THEORY

2.1. Crystal Structure

Most solids are crystalline with their atoms arranged in a regular manner with a simple lattice, such as body-center-cubic (bcc), face-center-cubic (fcc), and hexagonal closed packed (hcp). The main goal of this study is to explore the fcc crystal structure. Attraction and repulsive forces holds metal atoms together through the metal bond. The fcc

[1] Research Assistant
[2] Professor, Corresponding Author

  ISBN :978-2-35500-003-4

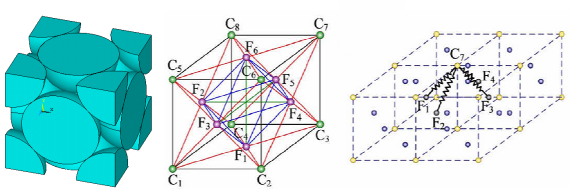

Figure 1.Simple-spring-single lattice model construction for the fcc structure and two springs sets which represented the center-corner by a red line; the corner to corner spring is represented by a black line.

bonding structure could be classified as the face-centered spring (with initial length r_0) and corner-corner springs (with initial length $2r_0\cos\theta$) as shown in Fig. 1. Both face-centered springs (as $C_1C_2\ldots C_iC_j$) and corner-corner springs (as C_1F_3 C_iF_j; $F_1F_3\ldots F_iF_j$) represent the interatomic forces between adjacent atoms. It results from the fact that the valence electrons (outer shell electrons) are not bound to a particular atom but are free to be shared by all of the atoms. In other words, they are delocalized in.

2.2. Finite element Method (FEM) and Atomistic-Continuum Method (ACM)

The beauty of the ACM methodology is the usage of the same model for tensile and vibration analysis. In ACM, the mass is the actual atomic mass, and the metal bonds are those obtained from the equivalent spring element. Therefore, in this research, modal analysis is also applied numerically to validate the experimental results. In this part of the analysis, the elementary theory of lateral vibration of beams was employed, and the relationship between natural frequencies and the Young's modulus of the beam was obtained. The results of both tensile and modal analyses were found to be reliable and acceptable [9]. One can generate the equations for a typical static constant-strain finite element. The total potential energy π_p is a function of the nodal displacement x, y, and z. Here, the total potential energy is given by Eq. (1)

$$\pi_p = U + \Omega_b + \Omega_p + \Omega_s \tag{1}$$

where U, Ω_b, Ω_p, and Ω_s represent the strain energy, the potential energy of the body force, the potential energy of the distributed, and the potential energy of the surface force load respectively. The above equation can be rewritten as a finite element integrated form as shown in Eq.(2):

Table 1. Parameters used in the Morse potential function

Metal	α [1/Å]	r_0[Å]	D[eV]
Pb	1.18	2.73	0.23
Ag	1.36	3.11	0.33
Ni	1.42	2.78	0.42
Cu	1.35	2.86	0.34
Al	1.16	3.25	0.27
Ca	0.80	4.56	0.16

$$\pi_p = \frac{1}{2}\iiint_v \{d\}^T[B]^T[D][B]\{d\}dV - \iiint_v \{d\}^T[N]^T\{F\}dV - \{d\}^T\{P\} - \iint_s \{d\}^T[N_s]^T\{T_s\}dS \tag{2}$$

where {d} represents the nodal displacement vector, [B] is the strain-displacement matrix, [D] is the modulus of the elasticity matrix, [N] is the shape function matrix, {F} is the body force vector, {P} is the external load vector, and $\{T_s\}$ is the traction force vector.

The ACM method transfers the interatomic potential function into a force-displacement curve to create an equivalent atomistic-continuum transfer element. Subsequently, the equivalent nanoscale model was analyzed by FEM. Compared with molecular dynamics, the ACM is more efficient, and it provides results quickly in an acceptable range. In this analysis, the following assumptions were established: First, the diatom binding energy was described by Morse potential function that has been adopted to describe the interatomic force for more than 70 years. The Morse potential describes the relationship of potential energy and diatom distance, and depicts the relationship of bond strength and diatom distance. Second, the crystal structures are under small deformation. Third, metallic bonding is the bonding between atoms within metals. It involves the delocalized sharing of free electrons among a lattice of metal atoms. Thus, the metallic bond may ignore the angle effect. Fourth, molecules are formed as atoms are held together with the bonds.

$$\varphi(r_{ij}) = D[e^{-2\alpha(r_{ij}-r_0)} - 2e^{-\alpha(r_{ij}-r_0)}] \tag{3}$$

where α and D are constants with dimensions of the reciprocal distance and energy, respectively, and r_0 is the equilibrium distance between two atoms. The constant used in the Morse potential function is shown in Table 1.

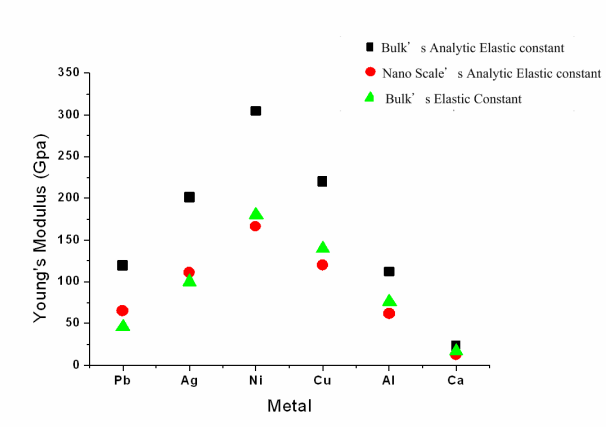

Figure 2. Analytic solution results of face center cubic in different kinds of metal.

Table 2. Young's modulus of FCC calculated in different lattice numbers.

Lattice number(n_x x n_y)	E_{Pb}	E_{Ag}	E_{Ni}	E_{Cu}
$1 \times 1_{(Bulk)}$[4]	119.33	201.00	304.36	220.24
$1 \times 1_{(Nano\text{-}scale)}$	64.80	110.41	166.18	120.15
3×3	54.18	91.53	138.38	100.11
6×6	51.05	86.11	130.29	94.27
10×10	49.75	83.86	126.93	91.84
100×100	47.94	80.75	122.27	88.48
1000×1000	47.75	80.43	121.80	88.14
10000×10000	47.74	80.40	121.75	88.10
100000×100000	47.73	80.40	121.75	88.10
Bulk Modulus	46.00	100.00	180.00	140.00

$$F_{bonds} = \frac{\partial E_{bond}}{\partial r} = 2\alpha D(-e^{-2\alpha(r_{ij}-r_0)} + e^{\alpha(r_{ij}-r_0)}) \quad (4)$$

The Young's modulus E could be estimated by the following equation:

$$E = \frac{\sigma}{\varepsilon} = \frac{F_{total}/A}{\Delta l / L} \quad (5)$$

where F_{total} is the total reaction force, ε represents the applied tensile strain loading which is the elongation per length, and A represents the equivalent area in the ACM.

2.3. SSSL Analytical Solution

The nanostructure is too small to experiment by tensile testing. Hence, some researchers apply modal analysis to investigate the mechanical properties of nanostructures [8]. The inter-atomic force and the position of atoms are respectively replaced by an equivalent spring element and nodes as shown in Fig. 1. The following are the distinct characteristics of a spring element as compared to a truss or a beam element: (1) has the same nature as of repulsive and attractive forces, (2) cannot resist bending moment, (3) has no cross-sectional area that needs to be defined, and (4) has a potential between atoms that is the same as the spring element. According to the two former characteristics, a spring element could represent a more realistic equivalent model since the chemical bond could neither be bent nor be defined by a cross-sectional area. This method could examine the nanostructures' mechanical properties with high computing efficiency.

In this thesis, the diatom binding energy was described by the Morse potential function. By comparing the results with existing bulk Young's modulus, it can be concluded that the present method can achieve the same results as other existing methods. Both analytical and numerical solutions were close to each other in this research. Equation 6 calculates the Young's modulus of the crystal structure.

$$E_{FCC} = 2\alpha^2 D\{[2(n_x + n_y) + 8n_x n_y]/4 + [(1 + n_x + n_y + 2n_x n_y)[2e^{-2\alpha r_0(\sqrt{2}-1)} - e^{-\alpha r_0(\sqrt{2}-1)}]]\} / (n_x n_y)\sqrt{2} r_0 \quad (6)$$

where n_x and n_y are respectively the number of lattices in the x and y directions. This model is basically a single cubic structure, though by the assumption of symmetric boundary conditions. Equation 6 is considered as an infinitely repeated cubic structure. If n_x and n_y approach infinity, the Young's modulus would come close to the bulk modulus as shown in Table 2. The data in Table 2 indicate that the neighbor lattice's bonding number will affect the Young's modulus significantly. The comparison of the Young's modulus of the face-centered-cubic in a single crystal structure can be divided into three categories: bulk analytic Young's modulus (calculated with the neighbor's lattice bonding, the same with the Chiang [4]), nano-scale analytic Young's modulus (without considering the neighbor's lattice bonding), and experimental bulk modulus as shown in Fig. 2. In Fig. 2,
the single crystal structure without considering the neighbor's lattice bonding leads to the bulk modulus.

3. SIMULATION RESULTS

3.1. Young's modulus of Copper by modal analysis and by tensile analysis

Copper is one of the most discussed materials in microelectro-mechanical and nanoelectro-mechanical systems (MEMS/NEMS). Hence, determining copper's mechanical properties is very important. This study

Table 3. Analysis of copper in (100), (110), and (111) direction results comparison

FCC Plane	(100)	(110)	(111)
Number of center to center	12	28	48
Number of corner to corner	5	10	13
Area of each plane nm^2	0.16	0.23	0.14
Elastic constant (Gpa)[8]	66.7	130.3	191.1
ANSYS elastic constant average(Gpa)	66.78	103.25	186.31

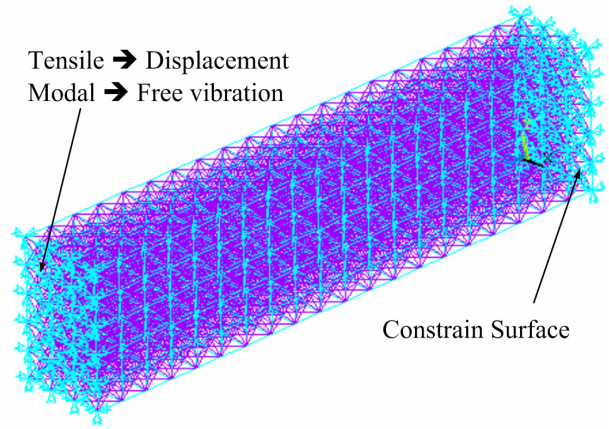

Figure 3. Boundary condition of the atomistic-continuum-transformation structure of face center cubic

compared the Young's modulus in different crystal planes of copper. In some research, they use the analytic solution from Generalized Hook's Law [8]. Meanwhile, this experiment used the atomistic-continuum method to calculate the Young's modulus. This is a comparative study of the Cu elastic constant which is in the (100), (110), and (111) crystal planes. The Young's modulus was calculated according to the crystal structure's bonding numbers and SSSL. The results are shown in Table 3, which reflects that different crystal planes will have different bonding numbers. The resulting Young's modulus is acceptable and is similar with the results of the Generalized Hook's Law. Figure 3 shows the ACM model and boundary condition of the crystal structure. This structure was built as a cantilever beam with a fixed end, while another side was given an external small displacement. The numerical model tested by the ANSYS® software obtained the reaction forces and natural frequency of the nanostructures, which could shed light on their mechanical properties. The size of the nanostructure is affected by the atoms' mechanical properties. This clearly showed that the there is a correlation between lattice numbers and elastic constant. It also shows that as the lattice numbers move closer to infinity, the Young's modulus would approach the bulk modulus. The more lattice numbers were calculated, the steadier elastic constant was obtained. By considering the atomic structure of copper, the mass of copper (M_{atom} = 1.05×10^{-25}kg) is assumed to be concentrated at the centers

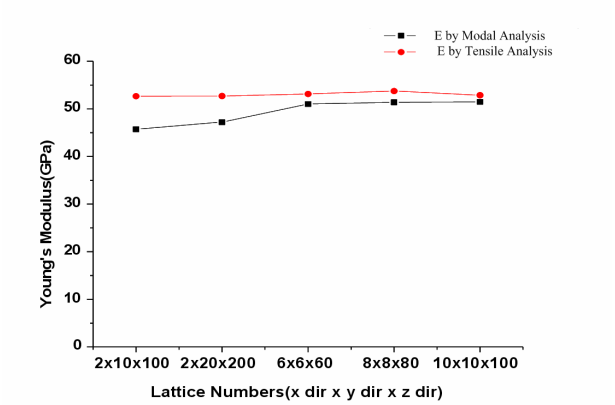

Figure 4. Analytic solution results of face-centered-cubic in different kinds of metal, and simulation results of the Young's modulus of copper in the same size by tensile and modal analyses

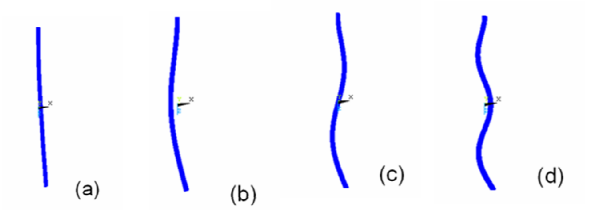

Figure 5. Mode Shape of atomic model: (a) first mode, (b) second mode, (c) third mode, (d) fourth mode

of atoms, which is equivalent to the mass of the nodes in the ACM model as the modal analysis is processed. Young's modulus could be calculated by the equation which is from the the Euler-Bernoulli beam theory. After the resonant frequency is calculated, the Young's modulus could be obtained by Eq. (7):

$$E = \frac{12\rho L^4 [\frac{2\pi f_1}{(1.875)^2}]^2}{t^2} \quad (7)$$

where $\rho = M_{atom}/V_{total} = N_{atom}m_{cu}/V_{total}$ is the density, N_{atom} is the number of atoms, m_{cu} is the mass of copper atom, $V_{total}$is the volume of the model, L represents the length, and f_1 represents the first resonant frequency of the crystal structure. In this analysis, when we adopted the same model in different crystal numbers to calculate the Young's modulus, we could obtain both modal analysis and tensile analysis; results have the same trend as shown in Figure 4. Figure 5 shows the mode shape of the atomic model. The other resonant frequency was obtained by obtaining the Young's modulus using the other equation for the other mode.

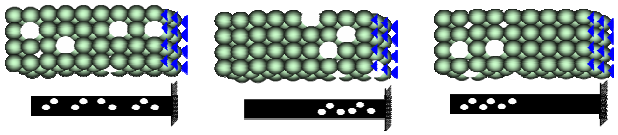

(a) (b) (c)

Figure 6. Three types of point defect distributed on the structure: (a) uniform distribution, (b) distribution on the fixed end, (c) distribution on the free end

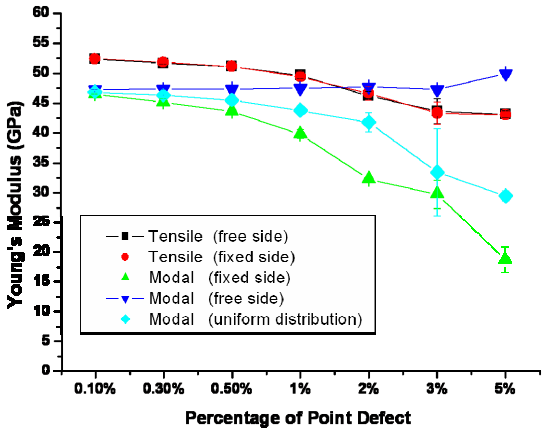

Figure 7. Percentage of point defects distribution that affects the simulation results of Young's modulus.

3.2. Young's modulus of Copper with point defects

A perfect crystal with every atom of the same type in the proper location does not exist. All crystals have some defect. As is already known, vacancy plays a major role in many kinds of point defects. Vacancy point defects analysis was based on the perfect crystal structure results. This section simulated and discussed the point defect distribution in three types as shown in Figure 6. One is the point defect distribution on the free side of the cantilever beam; the other is the point effect distribution on the fixed end, and the other is the point defects uniform distribution on the cantilever beam.

On the other hand, different kinds of defect and concentration of various vacancies affect the mechanical properties of crystal. The results of the tensile and modal analysis with the point defects of copper are shown in Fig. 7. Generally speaking, the Young's modulus will be changed by the percentage of point defect. The Young's modulus was observed to be higher with the tensile testing compared to the modal analysis. The Young's modulus increases as the point defect increases when the point defect distribution is on the free side. Because the point defects distribution is on such side, the model could increase the model frequency or decrease its stiffness. This is the reason why the point defects will increase the model frequency and the Young's modulus of the models at the same time. The study thus sought to determine if the point defect distribution could affect mechanical properties. The study carried out the following simulations: tensile testing and modal analysis.

4. CONCLUSION

In summary, the ACM atomic model was constructed using atomistic-continuum mechanics for application not only in axis tensile loading test but also in modal analysis. Both the tensile and modal analysis results were reliable and acceptable compared with the literature mentioned above. The simulation results of resonant frequency analysis agree with the analytical solution of the resonant frequency based on the Euler-Bernoulli beam theory. The size effect was observed at the nanoscale range from the atomistic model. The Young's modulus of the nanoscaled structure has size-dependent properties. In this research, comparing tensile and vibration analyses strongly suggests that the point defect distribution will affect the structure's mechanical properties. The most important finding from these data suggests that vacancy defect distribution concentrates at the free side of the specimen can provide adequate results. The ACM method simplifies the complexities of interaction forces among atoms while maintaining the calculation's accuracy and the computation efficiency. The results also reveal that the point defect distribution will affect the structure's mechanical properties. When the vacancy defect distribution is concentrated at the free end of the specimen, the Young's modulus increases. However, the point defects distributed on the fixed end will decrease the Young's modulus. According to the methodology of ACM, one could estimate the mechanical properties of a nanostructure with an appropriate potential energy. The crystal defects might be beneficial to examine in the future how the mechanical properties could be controlled by the point defects.

5. ACKNOWLEDGEMENT

The authors wish to thank the National Science Council of Taiwan R.O.C. for financially supporting this research under contract No. NSC 96-2221-E-007-070

6. REFERENCES

[1] V. B. Shenoy, R. Miller, E. B. Tadmor, D. Rodney, R. Phillips, M. Ortiz, "Quasicontinuum Models of Interfacial Structure and Deformation", Appl. Phys. Let., vol.80, 742-745, 1998.

[2] L. A. Girifalco, V. G. Weizer, “Application of the Morse Potential Function to Cubic Metals”, Phys. Rev., vol.114, 687–690, 1959.
[3] J. Rottler, D. J. Srolovitz, Roberto Car “Point defect dynamics in bcc metals”, Phys. Rev. B, vol.71, 064109, 2005.
[4] K. N. Chiang, C. Y. Chou, C. J. Wu, C. A. Yuan, “Prediction of The Bulk Elastic Constant of Metals Using Atomic-Level Single-Lattice Analytical Method”, Appl. Phys. Let. vol. 88, 171904-1-171904-2, 2006.
[5] C. J. Wu, C. Y. Chou, C. N. Han, K. N. Chiang, "Numerical Simulation of the Mechanical Properties of Carbon Nanotube Using the Atomistic-Continuum Mechanics.", European Nano System 2006, 14-15 December 2006, Paris, France.
[6] C. Y. Chou, C. Yuan, C. J. Wu, K. N. Chiang, “Numerical simulation of the mechanical properties of nanoscale metal clusters using the atomistic-continuum mechanics method.” NSTI EuroNanoSystem 2005, Paris (France), 2005.
[7] B. Liu, Y. Huang, S. Qu, K. C. Hwang, “The atomic–scale finite element method”, Comput.Methods Appl. Mech. Engrg., vol.193, 1849-1864, 2004.
[8] R. W. Hertzberg, Deformation and Fracture Mechanics of Engineering Materials, 4th edition. John Wiley & Sons, Inc. 1996.
[9] D. A. Hughes, N. Hansen, “Graded Nanostructures Produced by Sliding and Exhibiting Universal Behavior”, Phys. Rev. Let., vol.87,135503-1-135503-4, 2001.